Acta Cryst. (1996). D**52**, 623–630

Cryocrystallography of 3-Isopropylmalate Dehydrogenase from *Thermus thermophilus* and its Chimeric Enzyme

CHIKAHIRO NAGATA,[a] HIDEAKI MORIYAMA,[a] NOBUO TANAKA,[a] MASAYOSHI NAKASAKO,[b] MASAKI YAMAMOTO,[b] TATZUO UEKI[b] AND TAIRO OSHIMA[c]

[a]*Department of Life Science, Faculty of Bioscience and Biotechnology, Tokyo Institute of Technology, 4259 Nagatsuta-cho, Midori-ku, Yokohama, Kanagawa 226, Japan,* [b]*Biophysics Laboratory, The Institute of Physical and Chemical Research (RIKEN), 2–1 Hirosawa, Wako, Saitama 351–01, Japan, and* [c]*Department of Molecular Biology, Tokyo University of Pharmacy and Life Science, Horinouchi, Hachioji, Tokyo 192–03, Japan. E-mail: ntanaka@bio.titech.ac.jp*

(*Received 5 October 1995; accepted 7 December 1995*)

Abstract

The crystal structures of thermostable enzyme, 3-isopropylmalate dehydrogenase of *Thermus thermophilus* (10T) and a chimeric enzyme between *T. thermophilus* and *Bacillus subtilus* with one point mutation (cS82R), were determined at both 100 and 150 K. At the cryogenic condition, the volume of the unit cell decreased by 5% as a result of a contraction in the solvent region. Although the overall structures of both enzymes at low temperature were the same as that of 10T at room temperature, interactions between two domains and between two subunits in a functional dimer of cS82R were significantly altered. The decrease in the average temperature factor of 10T at low temperature and no significant decrease for cS82R suggested that the structure of the engineered enzyme (cS82R) may have many conformational substates even at low temperature, while the native enzyme (10T) at low temperature has a more definite conformation than that at room temperature. The location of water molecules around the enzyme molecule and the calculation of the radii of gyration suggested that cS82R had a weaker hydration than 10T.

1. Introduction

Studies on the thermostability of an enzyme are aimed at elucidating the fundamentals of folding of the protein, and producing more thermostable proteins for industrial purposes. Protein engineering has made it possible to produce a variety of chimeric proteins which inherit their parent's characters.

3-Isopropylmalate dehydrogenase (IPMDH, E.C. 1.1.1.85) is one of the enzymes which constitute the system of leucine biosynthesis. It catalyses both the dehydrogenation and decarboxylation of 3-isopropylmalate to 2-ketocaproate in the presence of divalent metal ions such as Mg^{2+} or Mn^{2+} (Yamada *et al.*, 1990). The functional unit is composed of two identical monomers (Fig. 1), between which an active site is located. The thermostability of the enzyme may be correlated with the growing temperature of the bacterium, since IPMDH derived from *Thermus thermophilus* (10T, hereafter) is more thermostable than any enzyme of the mesophile, in spite of the high sequence homology between them (Kagawa *et al.*, 1984; Kirino & Oshima, 1994; Kirino *et al.*, 1994). Chimeric enzymes between 10T and the enzyme of mesophilic *Bacilus subtilis* (10M, hereafter) were produced by connecting partial sequences of the two native enzymes, and were dedicated to the studies on the thermostabilities and three-dimensional structures (Numata *et al.*, 1995). 4M6T is constructed with residues 1–132 from 10M and residues 133–345 from 10T, and 2T2M6T has residues 73–132 from 10M, the remaining being from 10T. The measurement of activities indicated that 4M6T was more thermostable than 2T2M6T, though the former contains fewer parts of 10T. This measurement suggests that detailed structural studies are essential for the understanding of the thermostability of the enzyme. Decreased thermostability of the chimeric enzyme was found to be recovered by site-directed mutagenesis at the residue which the structure suggests to be involved with the thermostability (Tamakoshi, Yamagishi & Oshima, 1996). The structural studies on these enzymes have been undertaken to elucidate the relationships between their structures and thermostabilities (Imada *et al.*, 1991; Onodera *et al.*, 1994). The studies have concluded that each of the chimeric enzymes has the same structure as 10T except for the residues on the surface of the enzyme, and its thermostability may be recovered by releasing the stress in the molecule by mutation. However, in almost all cases, the crystal structures showed that larger temperature factors reduce some parts of the electron-density humps of the main chains. Therefore, it is difficult to understand the mechanism of thermostability of the enzyme. In cS82R, in which Ser82 of chimeric 2T2M6T (Fig. 2) was replaced by arginine, the residues around the 82nd residue were found to have a temperature factor larger than 60 $Å^2$ (Sakurai *et al.*, 1996).

Cryocrystallography has been developed for detailed structural studies on biological macromolecules. It is quite suitable for the study of protein crystals having large thermal vibrations at room temperature because it is expected that thermal vibrations decrease considerably at low temperature. In the present study, the structures of 10T and cS82R have been determined at 100 and 150 K. A detailed comparison of the structures determined at room temperature and low temperature will give an insight into the thermostability of IPMDH.

2. Materials and methods

2.1. *Preparation of the crystals*

The 10T and cS82R were prepared as described in previous papers (Yamada *et al.*, 1990: Sakurai *et al.*, 1996). Crystals were grown under the previously reported conditions with minor modification (Katsube, Tanaka, Takenaka, Yamada & Oshima, 1988; Sakurai *et al.*, 1992). Both crystals are bipyramidal and belong to the same space group of $P3_221$ with the similar cell dimensions as reported previously.

To carry out low-temperature experiments, the solvent in the crystal had to be replaced with solvent which contains cryoprotectant to protect from freezing. In the present study, glycerol was added as a cryoprotectant in the solution. However, as the dielectric and osmotic pressure shock destroyed the crystal lattice when the cryoprotectant was replaced quickly, dialysis against 10 m*M* HEPES, pH 7.5, 2.2 *M* ammonium sulfate and 22%(*w*/*v*) glycerol could be used to prepare suitable crystals for data collection at low temperature.

2.2. *Data collection*

Intensity data were collected by the oscillation method on an R-AXIS IIc diffractometer (Sato *et al.*, 1992). A rotating-anode X-ray generator (RU-200; Rigaku, Tokyo, Japan) was operated at 55 kV and 80 mA with a focus size of 3 × 0.3 mm. The Cu $K\alpha$ radiation was monochromated with an Ni filter and was focused on

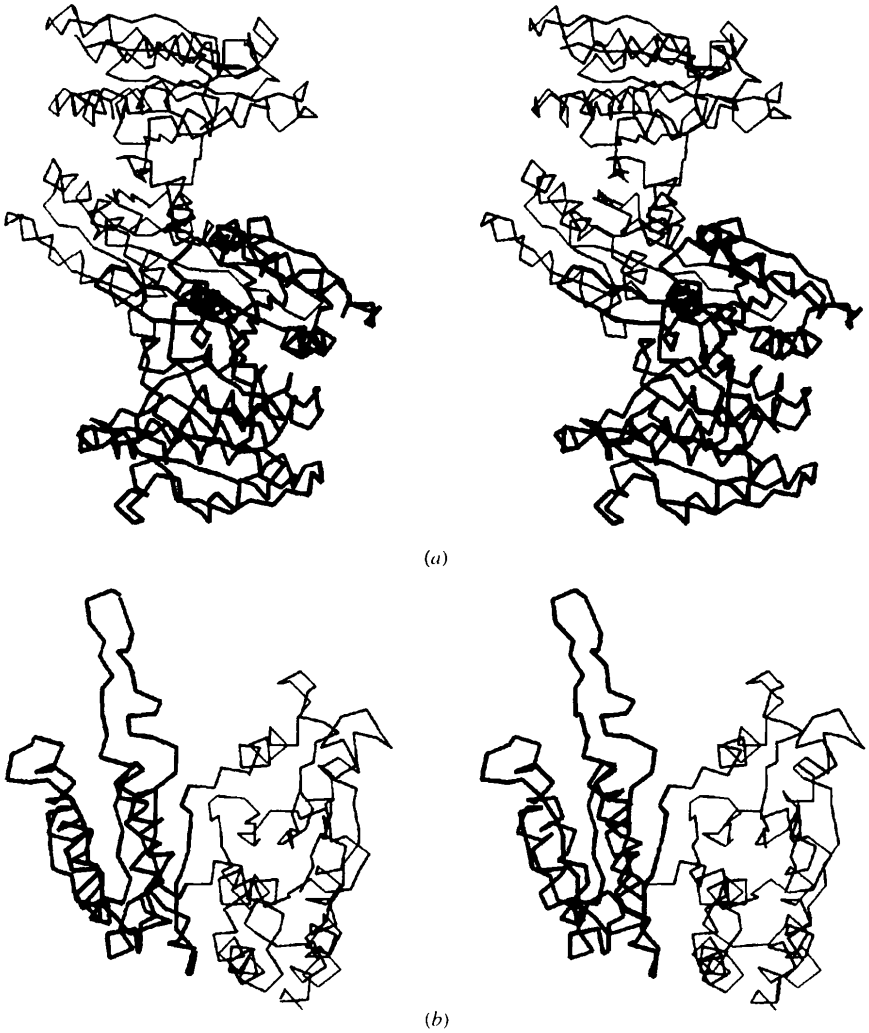

Fig. 1. Stereoscopic views of the Cα model of 10T IPMDH structure at 100 K. (*a*) A functional dimer composed of two identical subunits with crystallographic symmetry. Thick and thin lines represent each subunit of a dimer. (*b*) A subunit made of two domains. One consists of 99 residues from the N-terminus and residues from 252 to the C-terminus (thin line) and the other consists of residues 100–251 (thick line).

an imaging plate with two mirrors. A cryostream Cooler (Oxford Cryosystems, UK) was attached as a cooling unit, with the top of the nozzle fixed at a position within 1 cm from the mounted crystal. The crystal was mounted by surface tension of the mother liquid on a crystal mounting device, which was made of a slice of capillary tube, in order to decrease the absorption effect resulting from the crystal holder (Nakasako, Ueki, Toyoshima & Umeda, 1995). After fixing the mounting device on the goniometer of the R-AXIS IIc, the crystals were freezed by introducing cold nitrogen gas at 100 K by quickly opening the mechanical shutter at the outlet of air. 24 frames of oscillation photographs were taken to collect a complete data set under each set of conditions. Each frame scanned an oscillation angle of 1.5° with an exposure time of 1.5 h. After completing data collection at 100 K, the gas stream was warmed up at a rate of 120 K h^{-1} to produce data at 150 K from the same crystal, because no serious X-ray damage was detected with the 100 K data collection. During these measurements, the crystal was not removed from the goniometer to keep the orientation of the crystal and the distance between the crystal and the detector constant, which made it easy to compare the lattice parameters and structure at different temperatures. Even though the cryoprotectant was added, the diffraction of ice appeared and the diffraction from the protein crystal faded away when the crystal was warmed up beyond 150 K.

```
10T/cS82R    1  MKVAVLPGDG IGPEVTEAAL KVLRALDEAE GLGLAYEVFP FGGAAIDAFG
                 BBBBB       aaaaaaaaaaaaaaaaaaa      AAAAAA  bbbbbbb

10T         51  EPFPEPTRKG VEEAEAVLLG SVGGPKWDGL PRKIRPETGL LSLRKSQDLF
cS82R           EPFPEPTRKG VEEAEAVLLG SVGGPKWDQN PRELRPEKGL LSIRKQLDLF
                    cccccccc  CCCC                    ddddd ddddd    F

10T        101  ANLRPAKVFP GLERLSPLKE EIARGVDVLI VRELTGGIYF GEPRGMSEAE
cS82R           ANLRPVKVFE SLSDASPIRK EYIDNVDFVI VRELTGGIYF GEPRGMSEAE
                FFFFFFFFFF                GGGGGGGGG          KKKK  L

10T/cS82R   151  AWNTERYSKP EVERVARVAF EAARKRRKHV VSVDKANVLE VGEFWRKTVE
                 LLLLLLLLee eeeeeeeeee eeeee   II IIIII    f fffffffff

10T/cS82R   201  EVGRGYPDVA LEHQYVDAMA MHLVRSPARF DVVVTGNIFG DILSDLASVL
                 ffff   JJJ JJJJJggggg ggggg       HHHHHhhhh hhhhhhhhhh

10T/cS82R   251  PGSLGLLPSA SLGRGTPVFE PVHGSAPDIA GKGIANPTAA ILSAAMMLEH
                         EE EE    DDDDD                  iii iiiiiiii

10T/cS82R   301  AFGLVELARK VEDAVAKALL ETPPPDLGGS AGTEAFTATV LRHLA
                     jjjjjj jjjjjjjjjj j          kkkkkkkkk kkk
```

(*a*)

(*b*)

Fig. 2. (*a*) Amino-acid sequences of two IPMDH's. Residues which are not conserved between both enzymes are shown in the boxes. The secondary structures of 10T and cS82R are shown below the cS82R sequence, where upper case indicates β-strands and the lower case indicates α-helices. (*b*) Stereoscopic view of the Cα model of cS82R at 100 K. Thick lines represent the region from 74 to 133, which is a portion of mesophile enzyme, except for Arg82.

Table 1. *Statistics for data collection and refinement*

All crystals belong to the space group $P3_221$. V is the volume of the unit cell, calculated from the cell constants.

		10T			cS82R		
Data collection		100 K	150 K	293 K	100 K	150 K	293 K
$a = b$ (Å)		77.0	76.9	78.6*	77.3	77.4	78.9†
c (Å)		156.4	156.4	158.6*	157.1	156.8	158.4†
V (10^5 Å^3)		8.03	8.01	8.49	8.13	8.14	8.54
No. of unique reflections‡		19388	17504		22097	18560	
R_{merge}§		0.058	0.081		0.050	0.059	
Completeness (%)	2.5 Å	73.9	67.0		83.4	74.5	
	2.1 Å	59.8	53.9		67.2	56.4	
Mosaic spread (°)		0.28	0.46		0.31	0.36	
Refinement							
Resolution range (Å)		8.0–2.1	8.0–2.1		8.0–2.1	8.0–2.1	
No. of used reflections¶		18775	17351		21701	18210	
Final R factor		0.157	0.158		0.200	0.194	
R.m.s.d. bond lengths (Å)		0.015	0.015		0.017	0.017	
R.m.s.d. bond angles (°)		2.99	3.03		3.51	3.52	
No. of non-H atoms for refinement							
Protein		2595	2595	2595	2612	2612	2612
Waters		296	299	61*	243	219	79†

*From Imada *et al.* (1991). †From Sakurai *et al.* (1995). ‡The amplitude of the reflections for data collections larger than $1\sigma(F)$. §$R_{merge} = \sum_h \sum_i |I_i(h) - \langle I(h)\rangle| / \sum_h \sum_i (h)$. $I_i(h)$ is the intensity of the ith symmetry-related mate of the reflection h with the mean value $\langle I(h)\rangle$. ¶The amplitudes of the reflections used in the refinement are larger than $2\sigma(F)$.

Except for the temperature, all conditions of the measurement were the same as those at room temperature. Total reflections within a limited resolution were obtained by processing the imaging data frame with the program *PROCESS* (Higashi, 1990). The cell dimensions observed at 100 and 150 K compared with those at room temperature are given in Table 1. The conditions and statistics for the data collection are also listed in Table 1.

2.3. *Structure refinement*

The rigid-body refinement of the program *X-PLOR* (Brünger, 1992) was applied to locate the molecule correctly because of variations of the cell parameters for both crystals. In the case of 10T at 100 K, the molecule was easily located by this refinement with the data between 8.0 and 3.0 Å resolution, the R factor being decreased to 0.33. Simulated-annealing (SA) refinement and B-factor refinement were applied to the data between 8.0 and 2.1 Å. In the course of these refinements, several residues were not visible in the electron-density map in the connecting loop of β-strand C and α-helix d from Gly70 to Arg85, and on the surfaces which were far from the dimer interface. These residues were positioned in the omit map which was calculated during each refinement cycle. After the successive cycles of refinement, clear electron-density humps could be found for some residues including the those amino-acid residues which were ambiguous at the initial step. The omit map was also utilized to locate water molecules in the crystal. Location of interactive water molecules and modification of amino-acid residues were performed on the difference Fourier map and omit map using the graphics program *TURBO-FRODO* (Jones, 1985) on an Indigo2 workstation. Out of many peaks on the difference map, water molecules were assigned by considering their stereochemistry. At the final stage of the refinement, more than 200 water molecules were chosen which had temperature factors less than 60 Å^2. The final refinement converged the R factor to 0.16 for 18 775 reflections $[F > 2\sigma(F)]$ between 8.0 and 2.1 Å resolution. In the case of cS82R, the molecule could not be located in the cell by rigid-body refinement in which the target molecule was a whole subunit. An alternative refinement succeeded by introducing flexibility between the domains of the subunit. The R factor between 8.0 and 3.0 Å resolution was then reduced to 0.42. The SA refinement gave a molecule in which the domains have a slightly different orientation with respect to each other. After fitting the ambiguous residues on the omit map outlined above, and assigning water positions, the molecules were refined to converge the R factor to 0.20. The refinements of the structures at 150 K were performed by using the 100 K structures for both enzymes, because the cell parameters at 150 K were similar to those at 100 K.

The statistics for refinements were given in Table 1. After the refinements, the analyses of the results were mainly performed by using the program *FESTKOP* (Nakasako, unpublished work).

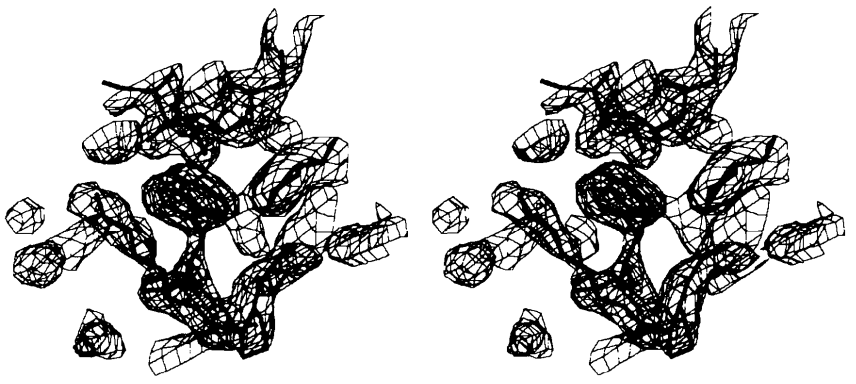

Fig. 3. Stereoscopic view of a representative portion of the $2|F_o| - |F_c|$ electron-density map at the C–d loop in cS82R at 100 K, contoured at 1.2σ level.

3. Results and discussion

Recent cryocrystallography developments have made it possible to discuss the detailed structures of a protein in relation to its function. Some highly disordered parts of the structure were ordered at low temperature and some residues on the surface of the molecule were visible in the electron-density map at low temperature, though they were not visible at room temperature. Especially, the polar and long side chains on the molecular surface which were oriented in a definite direction by the hydrogen bonds with water molecules or the other residues at low temperature.

The overall structures of both molecules, 10T and cS82R, at low temperature were topologically identical with those at room temperature. The molecule is a functional dimer, and each subunit consists of two domains. The residues which were not visible at room temperature were visible in the present study. The *C–d* loop from Gly70 to Arg85 were rebuilt with the omit map and could be located correctly (Fig. 3). Though Arg82 of cS82R made a hydrogen bond with Arg85 through a water molecule at room temperature, the electron density at 100 K suggested that the guanidyl group of Arg82 made a hydrogen bond with a water molecule, but it was too far from Arg85. On the other hand, Arg82 of 10T made a hydrogen bond directly with Arg85 (Fig. 4). These differences may be caused by the conformational change of the main chain at the *C–d* loop, because of the low sequence homology in the latter half of this loop (Fig. 2).

The structural comparison proved that the secondary structures were same in all molecules. The structure at 100 K was almost as same as that at 150 K. This result applied to both 10T and cS82R. By superposing a subunit at 100 K on the same one at 293 K, the deviations between the Cα atoms of each residue were calculated for both the enzymes, as plotted in Fig. 5. The average deviations of the subunit were 0.29 Å for 10T and 0.32 Å for cS82R, respectively. On the other hand, the average deviations of the other nonsuperposed subunit were 0.59 Å for 10T and 0.73 Å for cS82R, respectively. Each domain of the subunit at 100 K was also superposed on that at 293 K. When the first domains were superposed, the average deviations of the first and second domains were 0.30 and 0.28 Å for 10T, and 0.38

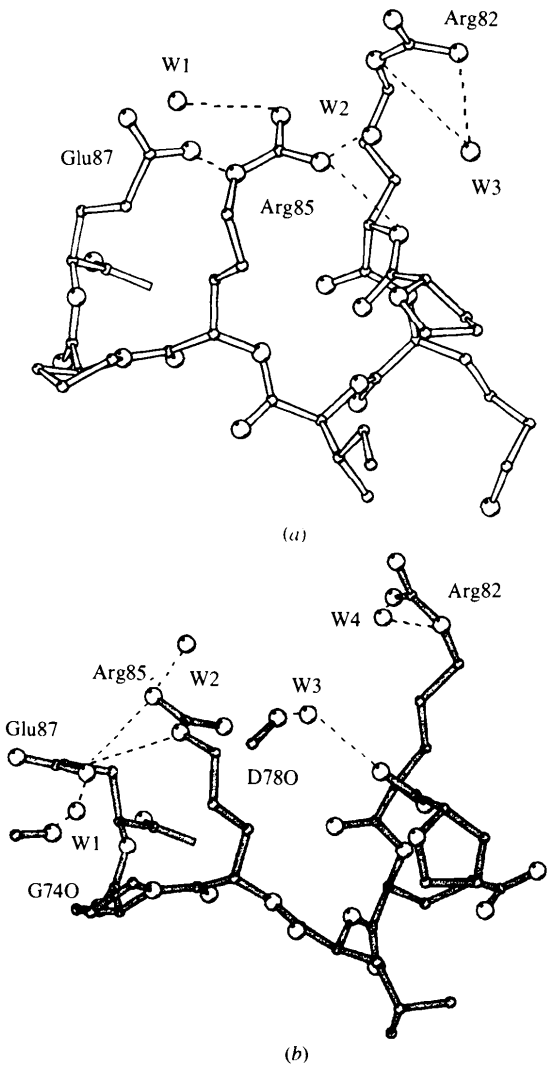

Fig. 4. Schematic drawing of the region around the Arg82 in (*a*) 10T determined at 100 K and (*b*) cS82R determined at 100 K. The dashed lines represent the hydrogen bonds.

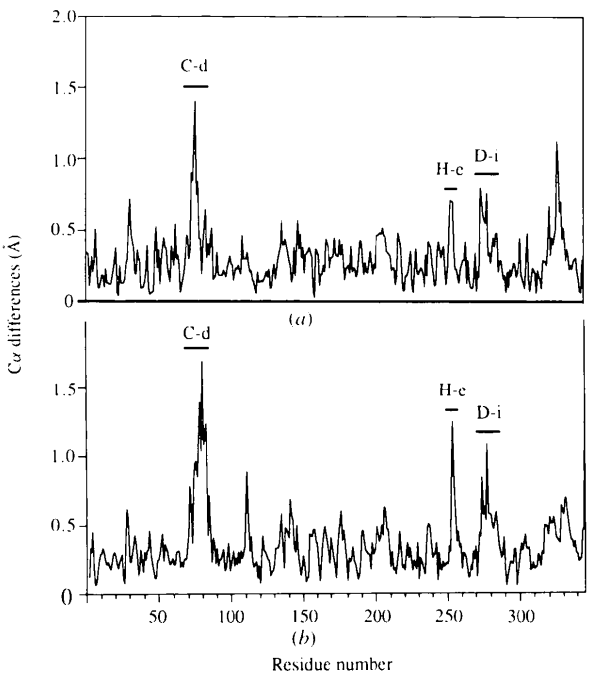

Fig. 5. Plots of the derivations of the Cα atoms of the amino-acid residues. (*a*) The deviations between Cα atoms in 10T determined at 100 K and 293 K. (*b*) Those of Cα atoms of cS82R determined at 100 K and 293 K

Table 2. *Averaged temperature factors (Å²)*

10T	293 K	150 K	100 K
All protein atoms	32.7	23.0	22.7
Main-chain atoms	32.0	21.7	21.3
Side-chain atoms	29.5	20.6	20.4
Water molecules	43.3	32.3	32.7
cS82R			
All protein atoms	34.7	34.0	33.1
Main-chain atoms	31.9	32.6	31.8
Side-chain atoms	33.6	35.4	34.6
Water molecules	45.8	38.4	40.7

and 0.31 Å for cS82R, respectively. When the second domains were superposed, the average deviations of the first and second domains were 0.26 and 0.32 Å for 10T, and 0.30 and 0.57 Å for cS82R, respectively. With respect to the central core of the molecule which is composed of the second domain of two subunits, the first domain of cS82R was rotated by 0.58° and was shifted by 1.13 Å, though the first domain of 10T was rotated by 0.53° and was shifted by 0.18 Å with the decrease of temperature. These results indicated that the structure of cS82R varied more than that of 10T when it was cooled. In Fig. 5, the larger deviations at low temperature were detected at the loop structure for both the enzymes. The deviations of the *C–d* loop were more than 1.4 Å, because of the high mobility of the loop or the possibility of the presence of varied conformations, judging from the high temperature factors at this loop. The *h–E* and *D–i* loops also deviated largely by 0.7 Å for 10T and 1.0 Å for cS82R, respectively. In spite of the large displacement at the loops, the secondary structures did not change their positions significantly. These results imply that the loop structure is altered within each loop so as to keep the chain folding identical at low temperature, with rearrangement of domains.

The temperature factors were plotted in Fig. 6, with the averaged temperature factors in Table 2, respectively. The larger temperature factors were found in the *C–d* loop region in both the enzymes even at 100 K. This reflects on the flexibility of the chain folding, which plays an important role on the catalytic reaction of the enzyme (Kadono *et al.*, 1996). Table 2 indicates that no serious decrease of the temperature factors was found in case of cS82R, although the temperature factors of 10T were decreased by about 10 Å² at 100 K. It may be plausible that cS82R has many conformational substates (Frauenfelder, Parak & Young, 1988) even at 100 K. But 10T decreases its thermal motion gradually at low temperature and as a result 10T has a definite conformation.

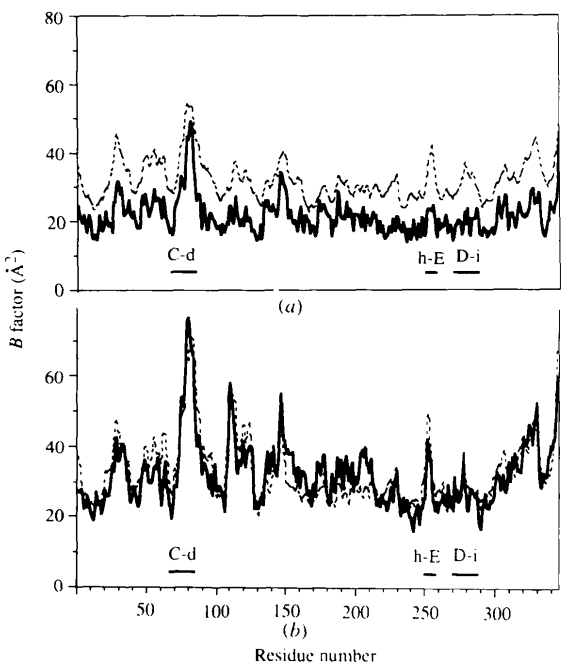

Fig. 6. The temperature factors of the amino-acid residues. The solid lines indicate those at 100 K and the dotted lines indicate those at 293 K. (*a*) 10T. (*b*) cS82R.

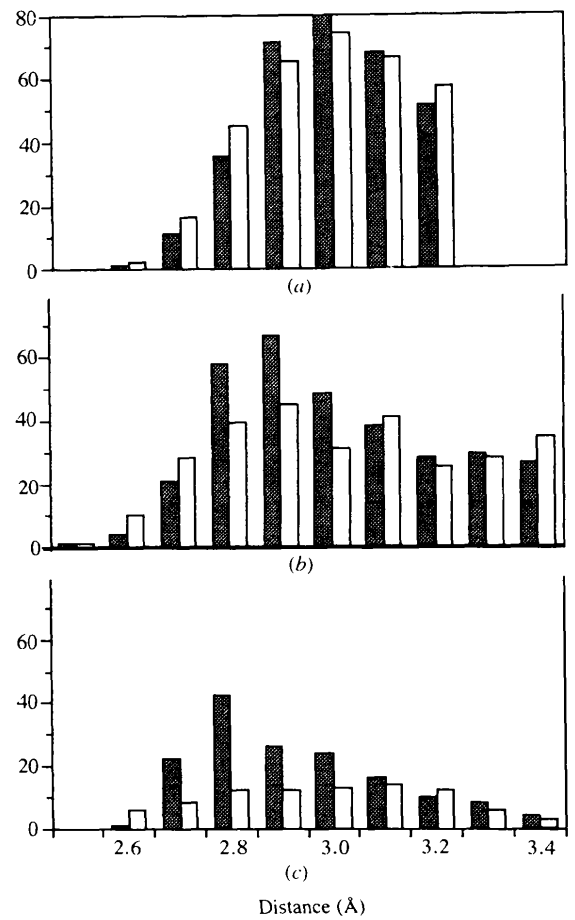

Fig. 7. Histogram of the hydrogen-bond distance between acceptor and donor within 2.4 and 3.4 Å for 10T (gray bars) and cS82R (white bars). (*a*) The protein–protein interaction. (*b*) The protein–water interaction. (*c*) The water–water interaction.

There were many water molecules in the crystal at low temperature as shown in Table 1. The numbers of hydrogen bonds between waters and between the protein and waters were 153 and 320 for the 10T, and 86 and 283 for the cS82R, respectively. The hydrogen-bond distances of protein–protein, protein–water and water–water interactions are plotted in Fig. 7. Though both the enzymes have a wide distribution of the distances of the hydrogen bonds between a protein and waters, the shorter distances were detected in 10T. This fact suggests the weaker interaction between cS82R and waters coupled with the fact that the enzyme has the larger temperature factors (Fig. 8).

The cell parameters of both enzymes were shortened by lowering the temperature. Though the parameters of 10T crystal were same as those of cS82R, the lengths of *a* axis of both enzymes were reduced by 1.6 Å which corresponds to 2.0% shrinkage. Also, the lengths of the *c* axis were reduced by 2.2 Å (1.4%) for 10T and by 1.3 Å (0.8%) for cS82R, respectively. These contraction of the cell parameters decreased the volume of the unit cell by 5.4% for 10T, and by 4.9% for cS82R, respectively. The shrinkage in volume was found in the crystals of RNase A (4.7%, Tilton, Dewan & Petsko, 1992), myoglobin (5.2%, Frauenfelder *et al.*, 1987) and lysozyme (4.8%, Young, Tilton & Dewan, 1994; 7.4%, Kurinov & Harrison, 1995). The shrinkage of the unit-cell volume was attributed to the contraction of the molecule and the cooling of thermal movement of water by lowering the temperature. The contraction of the molecule could be calculated from the atomic positions of the enzyme at different temperatures. From the positions of non-H atoms at 100 and 293 K, the thermal expansion coefficient is calculated with the equation described by Frauenfelder *et al.* (Frauenfelder *et al.*, 1987). The atomic coordinates at both temperatures derived the coefficients of 1.04×10^{-5} K^{-1} for 10T and 1.31×10^{-5} K^{-1} for cS82R, respectively. These values were not far from 5.0×10^{-5} K^{-1} for myoglobin (Fraunfelder *et al.*, 1987) and 4.0×10^{-5} K^{-1} for lysozyme (Kuronov & Harrison, 1995), respectively. In comparison with the shrinkages experimentally found for the unit cell which were by 5.4% for 10T and 4.9% for cS82R, the shrinkages of the molecule contributed to that of the unit cell by 0.20% for 10T and 0.25% for cS82R, respectively. These facts indicate that the shrinkage of the unit cell corresponds to the contract of the solvent region which is common by present in any protein crystals. The accurate positional parameters of the molecules make it possible to calculate the radius of gyration from atomic coordinates of each molecule. Table 3 shows that the radius of gyration of cS82R is bigger than that of 10T at any experimental temperature, even though it was calculated from a subunit or a dimer. The difference of radius between the two enzymes depends on the temperature, which means that the expansion of the subunit makes the enzyme less thermostable. For detailed discussions, the other chimeric enzymes need to be studied.*

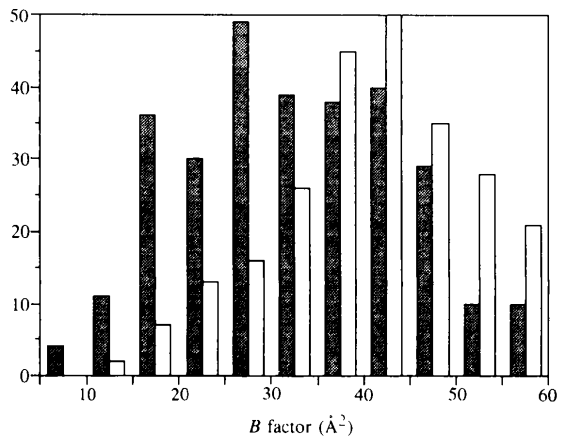

Fig. 8. Histogram of the number of water molecules *versus* the temperature factors for 10T (gray bars) and cS82R (white bars).

Table 3. *Radius of gyration (Å)*

The radii of gyration are calculated from the atomic coordinates of the refined structure.

	10T			cS82R		
	100 K	150 K	293 K	100 K	150 K	293 K
Subunit	20.36	20.37	20.39	20.38	20.41	20.48
Dimer	27.04	27.02	27.47	27.14	27.16	27.58

Authors express their thanks to the SR Structural Biology Research Group of RIKEN for their technical support and M. Sakurai and R. Hirose for their assistance with the purification and the crystallization. The present work was supported by a Grant-in-Aid for Scientific Research from the Ministry of Education Science and Culture of Japan (Nos. 05244102, 07304050 and 07280230).

* Atomic coordinates and structure factors have been deposited with the Protein Data Bank, Brookhaven National Laboratory (Reference: 1XAA, 1XAB, 1XAC, 1XAD, R1XAASF, R1XABSF, R1XACSF, R1XADSF). Free copies may be obtained through The Managing Editor, International Union of Crystallography, 5 Abbey Square, Chester CH1 2HU, England (Reference: AS0703).

References

Brünger, A. T. (1992). *X-PLOR. Version 3.0 Manual.* Yale University, New Haven, Connecticut, USA.

Frauenfelder, H., Hartmann, H., Karplus, M., Kuntz, I. D. Jr, Kuriyan, J., Parak, F., Petsko, G. A., Ringe, D., Tilton, R. F. Jr, Connolly, M. L. & Max, N. (1987). *Biochemistry*, **26**, 254–261.

Frauenfelder, H., Parak, F. & Young, R. D. (1988). *Ann. Rev. Biophys. Biophys. Chem.* **17**, 451–479.

Higashi, T. (1990). *J. Appl. Cryst.* **23**, 253–257.

Imada, K., Sato, M., Tanaka, N., Katsube, Y., Matsuura, Y. & Oshima, T. (1991). *J. Mol. Biol.* **222**, 725–738.

Jones, T. A. (1985). *Methods Enzymol.* **115**, 157–171.

Kadono, S., Sakurai, M., Moriyama, H., Sato, M., Hayashi, Y., Oshima, T. & Tanaka, N. (1996). *J. Biochem.* In the press.

Kagawa, Y., Nojima, H., Nukiwa, N., Ishikawa, M., Nakajima, T., Yasuhara, T., Tanaka, T. & Oshima, T. (1984). *J. Biol. Chem.* **259**, 2956–2960.

Katsube, Y., Tanaka, N., Takenaka, A., Yamada, T. & Oshima, T. (1988). *J. Biochem.* **104**, 679–680.

Kirino, H., Aoki, M., Aoshima, M., Hayashi, Y., Ohba, M., Yamagishi, A., Wakagi, T. & Oshima, T. (1994). *Eur. J. Biochem.* **220**, 275–281.

Kirino, H. & Oshima, T. (1994). *J. Biochem.* **109**, 852–857.

Kurinov, I. V. & Harrison, R. W. (1995). *Acta Cryst.* D**51**, 98–109.

Nakasako, M., Ueki, T., Toyoshima, C. & Umeda, Y. (1995). *J. Appl. Cryst.* **28**, 856–857.

Numata, N., Muro, M., Akutsu, N., Nosoh, Y., Yamagishi, A. & Oshima, T. (1995). *Protein Eng.* **8**, 39–43.

Onodera, K., Sakurai, M., Moriyama, H., Tanaka, N., Numata, K., Oshima, T., Sato, M. & Katsube, Y. (1994). *Protein Eng.* **7**, 453–459.

Sakurai, M., Moriyama, H., Onodera, K., Kadono, S., Numata, K., Hayashi, Y., Kawaguchi, J., Yamagishi, A., Oshima, T. & Tanaka, N. (1996). *Protein Eng.* In the press.

Sakurai, M., Onodera, K., Moriyama, H., Matsumoto, O., Tanaka, N., Numata, K., Imada, K., Sato, M., Katsube, Y. & Oshima, T. (1992). *J. Biochem.* **112**, 173–174.

Sato, M., Yamamoto, M., Imada, K., Katsube, Y., Tanaka, N. & Higashi, T. (1992). *J. Appl. Cryst.* **25**, 348–357.

Tamakoshi, M., Yamagishi, A. & Oshima, T. (1996). *Mol. Microbiol.* In the press.

Tilton, R. F., Dewan, J. C. & Petsko, G. A. (1992). *Biochemistry*, **31**, 2469–2481.

Yamada, T., Akutsu, N., Miyazaki, K., Kaminuma, K., Yoshida, M. & Oshima, T. (1990). *J. Biochem.* **108**, 449–456.

Young, A. C. M., Tilton, R. F. & Dewan, J. C. (1994). *J. Mol. Biol.* **235**, 302–317.